Energy Provisioning in Wireless Rechargeable Sensor Networks

Shibo He, Jiming Chen, *Senior Member, IEEE*, Fachang Jiang,
David K.Y. Yau, *Member, IEEE*, Guoliang Xing, *Member, IEEE*, and Youxian Sun

Abstract—Wireless rechargeable sensor networks (WRSNs) have emerged as an alternative to solving the challenges of size and operation time posed by traditional battery-powered systems. In this paper, we study a WRSN built from the industrial wireless identification and sensing platform (WISP) and commercial off-the-shelf RFID readers. The paper-thin WISP tags serve as sensors and can harvest energy from RF signals transmitted by the readers. This kind of WRSNs is highly desirable for indoor sensing and activity recognition and is gaining attention in the research community. One fundamental question in WRSN design is how to deploy readers in a network to ensure that the WISP tags can harvest sufficient energy for continuous operation. We refer to this issue as the *energy provisioning* problem. Based on a practical wireless recharge model supported by experimental data, we investigate two forms of the problem: *point provisioning* and *path provisioning*. Point provisioning uses the least number of readers to ensure that a static tag placed in *any* position of the network will receive a sufficient recharge rate for sustained operation. Path provisioning exploits the potential mobility of tags (e.g., those carried by human users) to further reduce the number of readers necessary: mobile tags can harvest excess energy in power-rich regions and store it for later use in power-deficient regions. Our analysis shows that our deployment methods, by exploiting the physical characteristics of wireless recharging, can greatly reduce the number of readers compared with those assuming traditional coverage models.

Index Terms—Wireless recharging, energy provisioning, sensor networks, WISP

✦

1 INTRODUCTION

WIRELESS sensor networks (WSNs) have found applications in a wide range of problems, from military surveillance to environmental monitoring, to disaster reliefs, and to home automation [1], [2]. In spite of their broad utility, however, energy efficiency remains a critical challenge for long network lifetime. Currently, most wireless sensor nodes are powered by batteries. The batteries add significant size and cost to the system, since battery technologies advance much more slowly than electronics in terms of volume efficiency. Therefore, battery-powered nodes have been found to be undesirable for embedded sensing such as structural health monitoring [3] and wearable sensing such as human activity recognition [4].

Battery-free systems aim to achieve perpetual network operation without the high operational overheads of replacing batteries from time to time [5], especially in harsh environments or where user convenience is paramount. One approach is to scavenge energy from surrounding energy sources. Known examples of energy sources include solar [6], vibrations [7], temperature variations [8], wind [9], biochemical processes [10], and passive human movements [11]. Getting rid of the batteries allows sensor nodes to be manufactured in small sizes. For example, the *Thermo Life* prototype [8] is of size about one-fourth of a penny coin, which is sufficiently small for many applications. The drawback of the energy scavenging approach, however, lies in its high reliance on unpredictable environmental conditions. For example, solar-powered nodes may fail to work if there is insufficient sunshine. Another approach of battery-free design is to distribute energy from energy-rich sources to energy-hungry nodes, which mainly involves two methods: 1) through strongly coupled magnetic resonances [12], and 2) through radio frequency (RF) signals [13]. Distributing energy through RF is highly desirable for ultralow-power applications such as ubiquitous sensing and computing. A well-known realization of this method is radio frequency identification (RFID) [14], where passive RFID tags attached to objects may reply with an electronic product code (EPC)-compliant ID when queried by a reader, by obtaining energy through the RF signal and reflecting the energy back.

The wireless identification and sensing platform (WISP) was developed by Intel to extend passive RFID beyond simple identification to include on-the-tag sensing and computing also [15]. WISP tags upload sensory data to querying readers via backscatter modulation. When they do so, they are also capable of harvesting energy from the RFID reader signals, thereby implementing a form of wireless recharging that is not available with traditional passive tags. The harvested surplus energy is stored in a capacitor and can be used for data sensing, logging, and computing when the readers are unavailable. A WISP tag of version *WISP4.1DL* made by our team according to Intel

- *S. He, J. Chen, F. Jiang, and Y. Sun are with the State Key Laboratory of Industrial Control Technology, Department of Control Science and Engineering, Zhejiang University, Hangzhou 310027, China. E-mail: {ferrer, fcjiang}@zju.edu.cn, {jmchen, yxsun}@iipc.zju.edu.cn.*
- *D.K.Y. Yau is with the Department of Computer Sciences, Purdue University, West Lafayette, IN 47907, and the Advanced Digital Sciences Center, Singapore. E-mail: yau@cs.purdue.edu.*
- *G. Xing is with the Department of Computer Science and Engineering, Michigan State University, 3115 Engineering Building, East Lansing, MI 48824-1226. E-mail: glxing@msu.edu.*
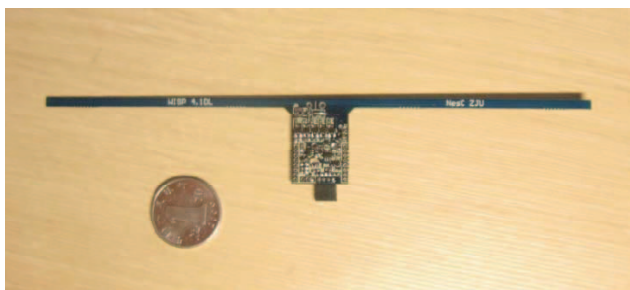
Fig. 1. Intel *WISP4.1DL*.

schematics is shown in Fig. 1. The *WISP 4.1DL* (excluding the antenna) is of similar size as a 10 cent coin; it can, thus, can be easily attached to objects or human bodies given suitable forms of the antenna (e.g., a pliable antenna like the one proposed in [13]).

The powered nature yet small size of WISP tags render them highly desirable for indoor sensing [13], and it has been shown that the WISP approach is superior to RFID for daily activity recognition [4]. Another example application is using the tags to continuously monitor the temperature of milk cartons [13]. In general, small header pins on the tags provide expansion ports to different daughter boards and external sensors; the thin tags can, thus, be used in diverse applications such as elderly care and smart homes, where they cooperate with supporting readers to form a *wireless rechargeable sensor network* (WRSN). Much research has focused on the design of traditional battery-based WSNs, but research on WRSNs has received relatively little attention.

In this paper, we treat readers as nodes in a wireless recharge infrastructure for a population of tags in a WRSN. One important design question is then the deployment of readers to guarantee perpetual operation of the tags. We refer to this as the *energy provisioning* problem. The problem is important to ensure system performance while minimizing the cost. On the one hand, we need to provision sufficient energy for the tags to run their tasks perpetually. On the other hand, we would like to deploy as few readers as possible, because a reader is significantly more expensive (more than 100 times) than a WISP tag.

We define two forms of the above energy provisioning problem: 1) *point provisioning* and 2) *path provisioning*. In point provisioning, the WISP tags are assumed to be static. In this case, readers should be deployed to ensure that, no matter where a tag is located in the network, its recharge rate (i.e., harvested energy per second) is no less than its average power consumption (i.e., energy consumed per second). In *path provisioning*, WISP tags are assumed to move because, for example, they are worn by human users or attached to other mobile entities. In this case, if a tag can gain energy only at a low rate along parts of its path, there may be no loss of sustained operation as long as the tag can harvest enough extra energy along other parts of the path and has a large enough capacitor to store the extra energy. The path provisioning then aims to determine how to deploy readers so that the average recharge rate of a tag over time is high enough to sustain its operation given the tag's mobility pattern.

To solve the aforementioned two kinds of provisioning in WRSNs, we have to first know the wireless recharge model of a WISP tag: a function of the tag's harvested energy per second given its distance from a reader. We propose a practical recharge model based on the well-known Friis's free space equation and utilize extensive experimental data to fit the parameters. The recharge model is a decreasing function of distance from the reader. Denote the threshold of the distance by r_1, at which the recharge power equals the average consumption power of the WISP tag. When the tag is located farther than r_1 from any reader, multiple readers can be used to guarantee the point provisioning of the tag. Thus, a further question is how multiple concurrent readers may impact the wireless recharging. We show through experimental data that the wireless recharge model is *additive*, in that the aggregate recharge power by multiple readers is equal to the sum of the magnitudes of recharge power of individual readers. We will also discuss the impact of mobility of WISP tags on the recharging using experimental data and demonstrate that the mobility can smooth out variable small-scale effects of radio waves due to surrounding factors.

Since the provisioning problem is about the placement of readers in relation to tags in a network, the problem can be related to the coverage problem in traditional WSNs. For sensor coverage, it is well known that if the sensing region is characterized as a disk of some radius, then deploying sensor nodes on the vertices of a triangular lattice yields the minimum number of nodes for covering a plane; we refer to this placement as "triangular deployment." Triangular deployment can be used as a basis for our point provisioning problem. However, instead of using a binary disk model, we will account for the fading of recharge signals in space. In addition, we exploit the additivity of the recharge model and utilize multiple readers to strengthen the energy provisioning of WISP tags. In *point provisioning*, we show that the side length of the equilateral triangular lattice can be significantly increased compared with the traditional triangular deployment, which means that the number of readers needed for a region of interest can be greatly reduced. We also analyze the asymptotic ratio of the required number of readers in our approach compared with the theoretically optimal. In *path provisioning*, we discuss how the mobility pattern will impact the deployment of readers and show how the side length of the traditional triangular deployment lattice can be further increased by exploiting the mobility. Our analysis is supported by extensive simulation results.

We emphasize that deploying a fixed infrastructure of wireless energy charging devices supporting potentially many small, possibly mobile tags is fundamentally different from deploying a fixed infrastructure of powered sensors and has the following important benefits: 1) the wireless recharge infrastructure is generic and can be reused for diverse types of tag sensors for different applications, and 2) more importantly, the tags, being inexpensive, extremely lightweight and small in size, and highly portable, can be easily and economically worn by many people, embedded extensively and unobstrusively in an infrastructure, or attached to many mobile objects for continuous sensing of their hosts.

The remainder of the paper is organized as follows: We discuss related work in Section 2. We formulate the energy provisioning problem in Section 3. Basic assumptions in our problem formulation are validated experimentally in Section 4. We propose solutions for the *point provisioning*

and *path provisioning* problems in Sections 5 and 6, respectively. In Section 7, we report simulation results to verify the analysis in our solution approaches. Section 8 concludes this paper.

2 RELATED WORK

Intel Research launched the WISP programme in 2005. Philipose et al. [16] are the first to introduce the concept of WISP and propose its design requirements and potential applications. Sample et al. [15] systematically describe the detailed design of WISP tags. They present the hardware and firmware architecture and discuss issues of power management, wireless charging, and sensor loading. They also give a WISP tag application of measuring environmental temperature. Buettner et al. [17] investigate characteristics of WSNs and WRSNs and argue that WRSNs have great potential in realizing "smart-dust" applications. In [13], a hardware architecture is proposed for WISP tags to continuously measure the temperature of milk cartons. The temperature of a carton can be continuously sampled and logged to external EEPROM if the difference between the current and latest logged values is above a predefined threshold. In [4], WISP tags are used to recognize the daily activities of people. It is shown that the WISP approach is advantageous over RFID-based approaches for the application [4]. Sample et al. [18] propose a novel method for integrating a capacitive touch interface into the architecture of traditional RFID tags without any change to the manufacturing process.

Since energy provisioning concerns the placement of readers relative to WISP tags, it is related to the fundamental coverage problem in WSNs. Traditional WSN coverage problems can be broadly put into two classes according to the sensing models. The first one assumes a perfect disk model and is referred to as *physical coverage*. In physical coverage, every point in a region of interest should be covered by at least one sensor node [19], [20]. It is shown in [21], [22] that the triangular deployment of sensor nodes on a plane obtains the smallest number of nodes to guarantee two-dimensional (2D) physical coverage. Another kind of WSN coverage is *information coverage*, sometimes also called *probabilistic coverage* because it assumes a probabilistic sensing model [23], [24]. In information coverage, first introduced by Wang et al. [23], a point is said to be covered as long as the joint information about it from multiple sensors exceeds a predefined threshold. Yang and Qiao [24] apply the concept of information coverage to the design of barrier coverage and show by simulations that the concept can prolong the network lifetime. Based on a probabilistic sensing model, Hefeeda and Ahmadi [25] propose an efficient protocol to select a subset of sensor nodes to cover a region of interest. According to the certainty of node locations, both physical and information coverage can be further divided into deterministic [26] and random deployments [27].

Our work determines the optimal number of RFID readers in deterministic deployments to satisfy the energy needs of either static WISP tags or tags moving according to a statistical model. It is unique by its focus on the characteristics of wireless recharging as motivated by the WISP platform. We design approximation algorithms for point provisioning and path provisioning. We derive analytically upper bound approximation ratios of our solutions to the optimal ones, thus bounding the worst-case distances of our solutions from the best possible. Our results will be compared and contrasted with those for physical coverage in traditional WSNs.

3 PRELIMINARIES AND PROBLEM STATEMENT

The Intel WISP tag is built on RFID technology and inherits the EPC Class 1 Generation 2 protocol. A WISP tag has an on-board ultralow-power 16-bit flash microcontroller, which manages energy harvesting, sensing, computation, and bidirectional UHF communication [17]. A tag cannot actively communicate with readers, nor with other WISP tags. It only responds with sensing data to a querying reader, and the data are of maximum size 64 bits per query. The latest hardware version *WISP4.1DL* by Intel includes 32 Kbytes of flash memory, 8 Kbytes of serial flash memory, an ADXL330 3-axis accelerometer, a temperature sensor, and a capacitance sensor.

WISP tags can work in an active or aquiescent state. As power consumption in the active state is much higher than that in the quiescent state, a WISP tag is typically in the sleep state most of the time and activated as necessary in an interrupt-driven manner. The active state mainly includes two processes: 1) sensing, computing, and data logging, and 2) communication with readers. When a reader wishes to download sensory data from a tag, it sends the tag a query command. The tag's external input pin interrupt will be triggered, which communicates any logged data in the tag to the reader. We assume that the tags are duty cycled periodically, and the period duration is T. Hence, every T time, a tag enters a sensing and data logging state by a timer interrupt and the state lasts for T_s time.

As aforementioned, the two processes in the active state can be performed independently. In many applications such as monitoring the quality of goods in a supply chain, the integrity of the monitored information is more critical than the delay of reporting this information to the readers. We are, thus, concerned with how to provide sufficient energy for WISP tags to achieve sustained operation of its sensing and data logging tasks and do not consider the communication process for transmitting sensory data to readers; we refer to this as the *energy provisioning* problem. We assume that there is a collection of WISP tags in a region of interest Ω and N off-the-shelf RFID readers are used to recharge them wirelessly. We assume that Ω is a sufficient large rectangular plane of side lengths l_1 and l_2. For communication, we assume that readers will come within range of a tag from time to time to upload data logged at the tag; the readers will supply the necessary energy during this reading process. Our objective is, therefore, the timely sensing and recording of dynamic data to avoid any information loss, whereas the data reporting is assumed to be delay tolerant so that it can occur in a batch manner. This paradigm fits many real-world applications such as daily logs of personal activity and health data to form long-term profiles of subjects. Denote the power consumption for sensing and data logging and sleeping in the quiescent state by p_s and p_q, respectively. Assume that the time duration for sensing and data logging per duty cycle is T_s. Let $\bar{p}_s = \frac{(T - T_s)p_q + T_s p_s}{T}$ and the average recharge power be p_a. When

$p_a \geq \bar{p}_s$, the tag can sustain its sensing and logging activities over time. We have the following definition of *energy provisioning* in the WRSN consisting of tags and readers.

Definition 1 (Energy provisioning). *A WISP tag, say i, is energy provisioned by readers in the WRSN if its average recharge power, p_a, satisfies $p_a \geq \bar{p}_s$. A WRSN is energy provisioned if every tag in it is energy provisioned.*

When the WRSN is energy provisioned, targets in the region of interest can be continuously monitored by the tags, and there is no missed information. This is similar to the *coverage* problem in traditional WSNs in which sensors are deployed to sufficiently monitor a region of interest. However, a key difference between the two problems is the direction of signal transmission: the tags in our problem are charged from RF signals transmitted from the readers to be deployed, while sensor nodes are deployed to sense the signal transmitted by targets in a traditional coverage problem. As the wireless recharge model of tags is fundamentally different from the sensing model of sensors, existing solutions to the coverage problem [22], [26] cannot be directly applied to the energy provisioning problem that we study in this work.

Depending on the application context, the WISP tags can be static (e.g., they are fixed to walls of a room) or mobile (e.g., they are worn by human users for activity monitoring). We refer to energy provisioning in these two cases as *point provisioning* and *path provisioning*, respectively. In point provisioning, we have to deploy readers to ensure that a tag in any location of the network is energy provisioned. This is important because any WISP tag can be guaranteed sustainable operation no matter where it is located. Formally, we define the problem as follows:

Point provisioning problem: Assume that there are N readers and a set of WISP tags in a 2D region Ω, the *point provisioning* problem determines how to deploy N readers such that

$$\min N \qquad \text{s.t. } p_a(x,y) \geq \bar{p}_s, \ \forall \ (x,y) \in \Omega, \qquad (1)$$

where $p_a(x,y)$ is the average recharge power for a tag placed at point (x,y) in the region Ω.

Different from *point provisioning*, where the tags are static, the tags can move in *path provisioning*. What matters in this case is the mobility pattern of the WISP tags, which affects how they may collect energy during the movement. Denote by $E(t)$ the cumulative energy that tag i harvests during time interval $[t_0, t]$. The *path provisioning* problem can be defined as follows:

Path provisioning problem: Assume that there are N readers and a set of WISP tags in a 2D region Ω, the *path provisioning* problem determines how to deploy N readers such that

$$\min N \qquad (2)$$

$$\text{s.t.} \quad \lim_{t \to \infty} \frac{E(t)}{t - t_0} \geq \bar{p}_s, \ \forall \ \text{every WISP tag in } \Omega. \quad (3)$$

In (3), the long-term average recharge rate is required to be no smaller than the power consumption of tags. In both the point and path energy provisioning problems, we have to determine the location of each reader so that the number of readers can be minimized, while the WISP tags can still be energy provisioned. Both the locations of the readers and the total number of readers are the variables to be optimized in the formulation.

4 EMPIRICAL WIRELESS RECHARGE MODEL

A critical factor impacting energy provisioning in WRSN is the wireless recharge model. In this section, we give practical models for the wireless recharge power when either a single reader or multiple readers are used in the recharge process. Moreover, we discuss the impact of tag mobility on the wireless recharge model.

4.1 Wireless Recharge Power of a Single Reader

When radio waves travel in space, their powers attenuate with increased travel distance. The simplest propagation model is free space propagation. According to Friis's free space equation, the receive power p_r of RF signal, d m away from the source power p_0, can be expressed as

$$p_r = G_s G_r \left(\frac{\lambda}{4\pi d}\right)^2 p_0,$$

where G_s is the source antenna gain, G_r is the receive antenna gain, and λ is the wavelength. Friis's equation is useful for long distance transmission such as satellite communication and often serves as a basic model for different applications. In WRSNs, readers transmit RF signals through circularly polarized antennas, and WISP tags receive the signal via linearly polarized dipole antennas. There exists polarization loss, which should be added to the basic Friis' equation. Moreover, the receive signal power should be rectified and converted to electrical energy before it can be used. Hence, we give an empirical model of wireless recharging in WRSNs as follows:

$$p_r = \frac{G_s G_r \eta}{L_p} \left(\frac{\lambda}{4\pi(d + \beta)}\right)^2 p_0, \qquad (4)$$

where L_p is polarization loss, η can be referred to as rectifier efficiency, and β is a parameter to adjust the Friis' free space equation for short distance transmission.

We perform experiments to verify if (4) is practical in our indoor environments. We use the *WISP4.1DL* tag shown in Fig. 1. The reader is a standard commercial RFID reader, *Impinj Octane3 Speedway*, with circularly polarized antennas, which have transmit gain $G_s = 8$ dBi. The transmit frequency of readers ranges between 920-925 MHz; thus, the average wavelength is about 0.33 m. The WISP tag has a linearly polarized dipole antenna and has receive gain $G_r = 2$ dBi according to [13]. To reduce multipath effects, we place the reader and WISP tag 0.58 m away from the floor. We let the antenna of the reader be parallel with the antenna of the tag to lessen orientation effects. The tag is programmed to be in the quiescent state for all the experiments to maximize the receive energy stored in the capacitor of capacitance $C = 100 \ \mu F$. We record the initial voltage V_i and final voltage V_f of the capacitor as well as the wireless recharge duration $\triangle t$. The wireless recharge power can be calculated by $\frac{C}{2\triangle t}(V_f^2 - V_i^2)$. The distance between the antennas of the reader and tag varies from 0.3 to 1.5 m in increments of 0.1 m. At each location, the recharge
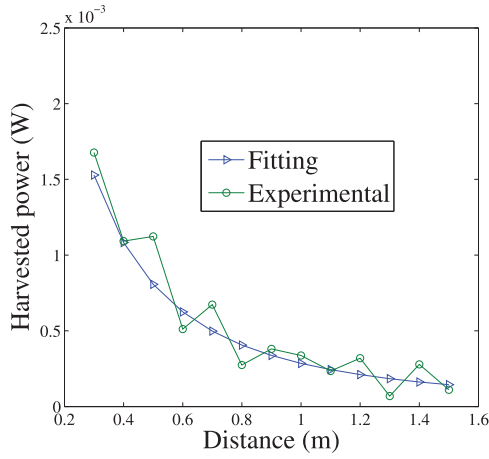
Fig. 2. Experimental and theoretical results for the rectified power under different distances from the source antenna of transmit power 1 W (30 dBm).

experiment is performed 10 times, and the average recharge power is plotted in Fig. 2 as marked by the circles.

We adopt (4) to fit the experimental data and obtain the rectified efficiency $\eta = 0.125$ and $\beta = 0.2316$. The fitting results are also depicted in Fig. 2 as marked by the triangles. We have three observations about the results: 1) There are small fluctuations in the experimental data because of small-scale effects such as multipath and occlusion. These small scale effects work differently at different locations, and impact the recharge power for the tags. However, from Fig. 2, we see that the experimental results closely approximate the fitting results most of the time. 2) Note that the rectified efficiency η obtained is much smaller than that reported in [13]. This is because we do not include multipath and occlusion effects in (4), and η in fact represents the rectified efficiency as well as the impact of the small scale effects. 3) In our experiments, we do not account for orientation effects of the antennas, which may affect the performance in actual applications. These effects will be reduced significantly when omnidirectional antennas for WISP tags are realized as planned for the next-generation design of the tags [13].

When a tag is far away from a reader, the tag antenna will receive negligible power of the reader's RF signals, which is hard to be rectified to useful electrical energy. We denote this threshold of negligible power by $\bar{p}_{th}$ and the corresponding distance from the reader by r_2. When $d > r_2$, we assume that $p_r = 0$. Hence, for a reader located at $(0,0)$, the wireless recharge power received by a tag at point (x, y) is given by

$$p_r(x,y) = \begin{cases} \dfrac{\tau}{(d+\beta)^2}, & d \le r_2 \\ 0, & d > r_2, \end{cases} \tag{5}$$

where $\tau = \frac{G_s G_r \eta}{L_p}\left(\frac{\lambda}{4\pi}\right)^2 p_0$, and $d = \sqrt{x^2 + y^2}$. From (5), r_2 and $\bar{p}_{th}$ have a relationship of $r_2 = \sqrt{\frac{\tau}{\bar{p}_{th}}} - \beta$. Let $r_1 = \sqrt{\frac{\tau}{\bar{p}_s}} - \beta$ denote the range within which a single reader can provision sufficient energy for the tag's operation. In certain actual applications, it is possible that $r_2 \gg r_1$. In this case, we discuss how additive power from multiple readers can be used to extend the operation range.

4.2 Wireless Recharge Power of Multiple Readers

The previous section discusses wireless recharge by one reader. A single reader (with an antenna) cannot provision adequate energy for tag locations, where the available recharge power is smaller than the average consumption power $\bar{p}_s$ of the tag. In this case, multiple readers are needed for the energy provisioning.

The basic question about using multiple readers is how their wireless recharge power will aggregate at a specific location. Intuitively, the recharge power at a specific location is simply the sum of the individual recharge power of each reader. To verify this, we place two readers (more precisely, two antennas connected to two readers) facing each other and put a WISP tag in the middle between them. The experiment setting is the same as in Section 4.1. The distance between the tag and either reader varies from 0.6 to 1.2 m in increments of 0.1 m. The wireless recharge results are given in Table 1. The second row of Table 1 records the recharge power from reader 1 when reader 2 is turned off. The third row gives the opposite case when reader 2 is on but reader 1 is off. The fourth row gives the sum of the values in the second and third rows. The fifth row records the measured recharge power when both the readers are on, which we refer to as the joint recharge power. The last row calculates the relative errors between the sum of the individual recharge power and the joint recharge power.

We can see from Table 1 that the relative errors are small between the sum of the individual recharge power and the joint recharge power when the distance $d = 0.9, 1.0, 1.1, 1.2$m. When the distance is smaller, the relative errors are a bit larger. This is likely due to the charging property of the capacitor. Note also that the recharge power of reader 2 at each location is a little different from that of reader 1. This is because the different placements of the readers result in different small-scale effects.

From the above observations, we assume that the wireless recharge power received by a WISP tag from multiple readers is additive, especially when the distances

TABLE 1
Additivity of the Transmission Power of Two Readers

Rectified power (W)/distance (m)	1.2	1.1	1.0	0.9	0.8	0.7	0.6
Reader 1	2.09×10^{-4}	1.68×10^{-4}	2.48×10^{-4}	3.56×10^{-4}	3.28×10^{-4}	6.78×10^{-4}	4.90×10^{-4}
Reader 2	2.43×10^{-4}	1.15×10^{-4}	3.21×10^{-4}	2.47×10^{-4}	2.37×10^{-4}	5.01×10^{-4}	4.43×10^{-4}
Sum of Reader 1 and Reader 2	4.52×10^{-4}	2.83×10^{-4}	5.69×10^{-4}	6.03×10^{-4}	5.66×10^{-4}	1.179×10^{-3}	9.34×10^{-4}
Readers 1 and 2	4.64×10^{-4}	2.58×10^{-4}	5.93×10^{-4}	5.91×10^{-4}	4.95×10^{-4}	9.98×10^{-4}	7.74×10^{-4}
Relative error	-0.0266	0.0891	-0.0426	0.0206	0.1251	0.1534	0.1711

from the readers are not too small, which corresponds to the targeted operation regime of multiple readers. From now on, we will denote the recharge power at location (x, y) from reader i by $p_r^{(i)}(x, y)$ and the joint recharge power still by $p_r(x, y)$. When the specific reader is not important, we denote the recharge power at (x, y) simply by $p_r(x, y)$.

4.3 Impact of Mobility

In principle, the mobility of tags will impact the recharge power. The relative movement between readers and tags will cause Doppler shifts of the RF signals, thus affecting the receive channel frequency. The resultant frequency change is $f_c = v \cos \theta / \lambda$, where θ is the angle between the direction of the signal path and that of the relative movement, v is the velocity, and λ is the wavelength. In WRSN applications, people or objects carrying the tags typically move at low-to-moderate velocities. The resulting Doppler shift will, therefore, be small, and in this paper, we will exclude its influence in the recharge model.

As mentioned in Section 4.1, there are small variations of recharge power between locations due to small-scale (e.g., multipath) effects. One advantage of mobile tags is that they can smooth out the impact of these effects. This is because the total energy WISP tags harvest along a path depends on the average power along the path, which smooths out detailed dependencies on the surrounding factors. Take the experimental data in Section 4.1 for example. We show the recharge power for 13 locations shown in Fig. 2. We assume that the average recharge power at each location, say j, is the average over the data of locations $j-1$, j, and $j+1$ (for the first and last locations, we simply use the average of two locations), $j = 1, 2, \ldots, 13$. The average recharge power and the fitting recharge model obtained in the previous section are shown in Fig. 3. Clearly, the curve of the average experimental recharge power is smoother than that of the raw data, and it fits the model better.

5 POINT PROVISIONING

In this section, we focus on deploying readers to ensure point provisioning.

Before presenting our main results, we report two preliminary findings:

1. We introduce a revised recharge function, $\widetilde{p}_r(x, y)$, which is equivalent to (5):

    $$\widetilde{p}_r(x, y) = \begin{cases} \bar{p}_s, & d \leq r_1 \\ \dfrac{\tau}{(d + \beta)^2}, & r_1 \leq d \leq r_2 \\ 0, & d > r_2, \end{cases} \quad (6)$$

    where $r_1 = \sqrt{\frac{\tau}{\bar{p}_s}} - \beta$ can be regarded as the threshold distance within which the recharge power is larger than the average power consumption $\bar{p}_s$. A point (x, y) is energy provisioned whenever $p_r(x, y) \geq \bar{p}_s$. Hence, setting $\widetilde{p}_r(x, y) = \bar{p}_s$ when $p_r(x, y) \geq \bar{p}_s$ will not affect our main results. Where there is no confusion, we still use $p_r(x, y)$ to denote the revised recharge function in this section.

2. We introduce a new optimization problem that is equivalent to the point provisioning problem (1):
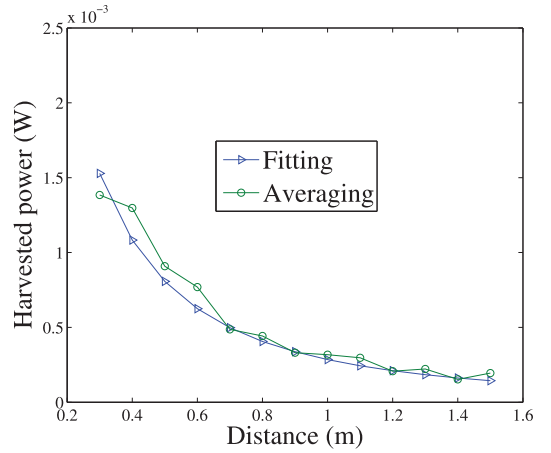

Fig. 3. The average recharge power and the fitting model of the recharge power, under transmit power of 1 W (30 dBm) and different distances from the reader.

$$\min \quad \iint_\Omega \sum_{i=1}^N p_r^{(i)}(x, y) dx \, dy \quad (7)$$

$$\text{s.t.} \quad \sum_{i=1}^N p_r^{(i)}(x, y) \geq \bar{p}_s. \quad (8)$$

Because the region Ω is assumed to be sufficiently large and can be taken as a plane,

$$\iint_\Omega p_r^{(i)}(x, y) dx \, dy$$

$$= \iint_\Omega \frac{\tau}{\left(\sqrt{(x - x_i)^2 + (y - y_i)^2} + \beta \right)^2} dx \, dy$$

$$= \iint_\Omega \frac{\tau}{\left(\sqrt{x^2 + y^2} + \beta \right)^2} dx \, dy$$

$$= \iint_\Omega p_r^{(j)}(x, y) dx \, dy, \forall i, j = 1, 2, \ldots, N.$$

Here, (x_i, y_i) is the position of reader i. Problem (7) is equivalent to Problem (1) because 1) $\min N$ is equivalent to $\min N\xi$, where $\xi = \int \int_\Omega p_r^{(1)}(x, y) dx \, dy$ is a constant, and 2) $N \int \int_\Omega p_r^{(1)}(x, y) dx \, dy = \int \int_\Omega \sum_{i=1}^N p_r^{(i)}(x, y) dx \, dy$.

In traditional WSNs, the sensors are typically assumed to fit a perfect disc sensing model, i.e., the points within the sensing range of a sensor are considered to be fully covered, while those beyond the sensing range are not covered at all. It is well known that according to the perfect disc sensing model, deploying sensor nodes on the vertices of equilateral triangles obtains the minimum number of nodes to ensure full coverage of a plane [22], [26]. In our problem, the recharge power received by a tag is a decreasing function of the distance between the tag and the reader that charges it, and the power received from different readers is additive at the same tag. These properties make our problem fundamentally different from the coverage problem in traditional WSNs. If we disregard the joint recharge power of multiple readers and set $p_r = 0$ when $d > r_1$, we can adopt the triangular deployment solution as it is to give
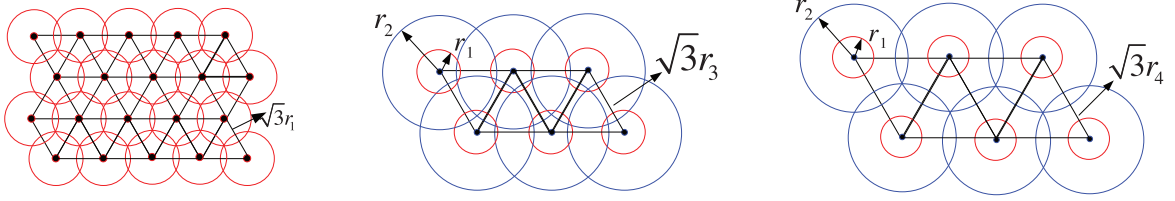
(a) Point provisioning under traditional disk model. (b) Point provisioning under our proposed method. (c) Path provisioning under our proposed method.

Fig. 4. Illustrations of point provisioning and path provisioning under our proposed methods and the traditional (conservative) triangular placement.

a conservative deployment for point provisioning, where the side length of the triangles is set to be $\sqrt{3}r_1$ (see Fig. 4a).

When additive recharge power is considered, however, a point that cannot be energy provisioned by a single reader can be energy provisioned by multiple readers. Hence, additivity can be exploited to reduce the number of readers for point provisioning. An interesting question is how much we can extend the side length of the equilateral triangles in the traditional triangular deployment while still guaranteeing energy provisioning. An illustration is shown in Fig. 4b. As it is quite difficult to obtain the minimum number of readers needed for point provisioning (the truly optimal solution), we estimate a lower bound of the optimal solution and provide an approximation ratio of our solution to this lower bound (i.e., the ratio gives the worst-case distance of our solution from the true optimal but the actual distance can be in fact shorter). We have the following theorem:

Theorem 1. *Under additive recharge power, the side length of equilateral triangles in the triangular deployment can be increased from $\sqrt{3}r_1$ to $\sqrt{3}r_3$ without losing point provisioning, where $r_3 = \sqrt{\frac{3\tau}{\bar{p}_s}} - \beta$. The corresponding required number of readers is denoted by N_a. Let N_* denote the minimum number of readers to ensure full point provisioning. When the dimensions of the rectangular region of interest increase to infinity, i.e., $l_1 \to \infty$ and $l_2 \to \infty$, we have*

$$\lim_{l_1 \to \infty, l_2 \to \infty} \frac{N_a}{N_*} \le \frac{\xi}{\bar{p}_s S_3}, \qquad (9)$$

where $S_3 = \frac{3\sqrt{3}r_3^2}{2}$, and ξ is given by

$$\xi = \pi r_1^2 \bar{p}_s + 2\pi\tau \ln \frac{r_2 + \beta}{r_1 + \beta} - 2\pi\tau\beta \frac{r_2 - r_1}{(r_1 + \beta)(r_2 + \beta)}.$$

Proof. Please see the proof in the Appendix, which can be found on the Computer Society Digital Library at http://doi.ieeecomputersociety.org/10.1109/TMC.2012.161. □

Remarks. *1) From Theorem 1, we know that the asymptotic approximation ratio of the triangular deployment to the theoretically optimal deployment is bounded by $\frac{\xi}{\bar{p}_s S_3}$. Our simulation results show that we can achieve good approximation ratios in the experiments. Furthermore, note that such a bound is not tight, and thus, the actual performance of our algorithm can be even better. 2) In the proof, we exclude the recharge power from readers on the vertices of other triangles. There are two reasons. First, we can decompose the problem and consider only a subregion of an equilateral triangle, which greatly simplifies the problem. Second, as r_1 and r_2 vary for different applications, it is infeasible, for general r_1 and r_2, to*

decide which readers from vertices of other triangles will impact the joint recharge power at the point inside the region of the considered triangle. For the same reasons, we make the same simplification for the analysis of path provisioning also.

6 PATH PROVISIONING

In this section, we are concerned with path provisioning, where WISP tags are assumed to move. As the distribution of recharge power over region Ω due to the deployed readers is not uniform (e.g., the points near readers have higher recharge power than those far away from the readers), the tags can gain surplus energy in power-rich regions, which can be used to compensate for the needs in power-hungry regions. Hence, mobility can be further exploited to reduce the number of readers for energy provisioning.

In the definition of path provisioning, we analyze the average recharge power as $t \to \infty$, which means that the tags can operate perpetually after a certain initial time. Assume that until time t, a tag has spent $t(x, y)$ time at location (x, y). The energy collected at (x, y) can be calculated by $\sum_{i=1}^{N} p_r^{(i)}(x, y)t(x, y)$. Hence, the path provisioning problem can be rewritten as follows:

$$\min N \qquad (10)$$

$$\text{s.t.} \lim_{t \to \infty} \frac{1}{t - t_0} \int \int_\Omega \sum_{i=1}^{N} p_r^{(i)}(x, y)t(x, y)dx\, dy \ge \bar{p}_s. \qquad (11)$$

There are three issues about path provisioning. The first is the mobility pattern of tags. From (11), the cumulative time $t(x, y)$ that a tag spends at location (x, y) greatly affects the average recharge power and, thus, the deployment of readers. The fraction $\lim_{t \to \infty} \frac{t(x,y)}{t-t_0}$ is referred to as the node distribution in [28], i.e., with what probability a tag will stay at a specific location. Let $f(x, y) = \lim_{t \to \infty} \frac{t(x,y)}{t-t_0}$, (11) can be rewritten as

$$\int \int_\Omega \sum_{i=1}^{N} p_r^{(i)}(x, y)f(x, y)dx\, dy \ge \bar{p}_s, \qquad (12)$$

which is much easier to handle than (11). There has been much work on the derivation of node distribution for certain well-known mobility models such as random waypoint [28]. Distributions from these models, from empirical measurements, or from knowledge of the specific mobility patterns can be used to drive the network design. For illustration in this paper, we assume that the node distribution follows the uniform distribution, i.e., $f(x, y) = \frac{1}{|\Omega|}$.
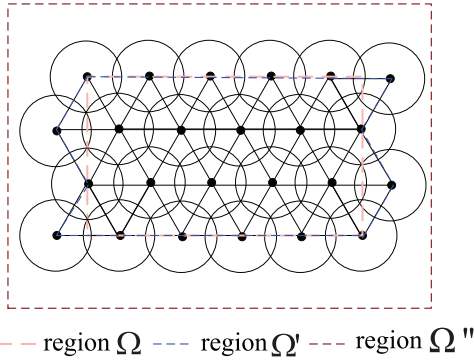
— — region Ω --- region Ω' --- region Ω''

Fig. 5. An illustration of region Ω, Ω', and Ω''.

The second issue concerns the deployment of readers. Different mobility behaviors will lead to different strategies of deployment. It is beyond the scope of this paper to investigate the detailed strategies. Rather, in this section, we will start from the triangular deployment proposed for point provisioning and show how the mobility can be exploited to further reduce the number of readers.

The third and last issue is how to calculate the average recharge power over region Ω. If we add some readers near the boundary of the region, the whole region Ω can be covered by a set of equilateral triangles, denoted by Ω' (see Fig. 5). As we assume that Ω is sufficiently large, and thus, $l_1, l_2 \gg r_2$, $\Omega \approx \Omega'$. For this reason, we consider region Ω' instead of Ω for simplicity of exposition. Assume that there are J triangles covering the region Ω'. Equation (12) can be calculated as

$$\sum_{j=1}^{J} \iint_{\Delta_j} \sum_{i=1}^{3} p_r^{(j_i)}(x,y) \frac{1}{|\Omega'|} dx\, dy \geq \bar{p}_s, \qquad (13)$$

where $|\Omega'|$ is the area of region Ω', Δ_j is the subregion inside triangle j, and $j_i, i = 1, 2, 3$, are the corresponding readers on the vertices of triangle j. (As discussed in the previous section, we exclude the recharge power from readers of other triangles).

Given the above discussions, we have the following theorem.

Theorem 2 (Uniform node distribution). *Assume that the node distribution is uniform. To ensure path provisioning of the region Ω' by triangular deployment, the side length of triangles can be further extended from $\sqrt{3}r_3$ to $\sqrt{3}r_4$, where $\sqrt{3}r_4$ is the maximum side length of triangles satisfying*

$$\frac{3}{|\Delta|} \int_0^{\frac{\pi}{3}} \int_0^{\frac{3r_4}{2\sin(\theta+\frac{\pi}{3})}} \frac{\tau}{(r+\beta)^2} r dr\, d\theta \geq \bar{p}_s, \qquad (14)$$

where $|\Delta|$ is the area of the equilateral triangle. Denote the corresponding required number of readers by N_a and the minimum number of readers by N_*. We have

$$\lim_{l_1 \to \infty, l_2 \to \infty} \frac{N_a}{N_*} \leq \frac{\zeta}{\bar{p}_s S_4}, \qquad (15)$$

where $S_4 = \frac{3\sqrt{3}r_4^2}{2}$, and ζ is given by

$$\zeta = 2\pi\tau \ln \frac{r_2+\beta}{\beta} - 2\pi\tau \frac{r_2}{r_2+\beta}.$$

Proof. As the node distribution is uniform, for each triangle i, the integration $\int \int_{\Delta_j} \sum_{i=1}^{3} p_r^{(j_i)}(x,y) dx\, dy$, $j = 1, 2, \ldots, J$, has the same value. Moreover, due to the symmetry of the three readers at the vertices of each triangle, the following equation holds:

$$\iint_{\Delta_j} p_r^{(j_{i_1})}(x,y) dx\, dy = \iint_{\Delta_j} p_r^{(j_{i_2})}(x,y) dx\, dy, \qquad (16)$$
$$i_1, i_2 = 1, 2, 3, \; j = 1, 2, \ldots, J.$$

Note that $J = \frac{|\Omega'|}{|\Delta_j|}$ and

$$\iint_{\Delta} p_r^{(j_1)}(x,y) dx\, dy = \int_0^{\frac{\pi}{3}} \int_0^{\frac{3r_4}{2\sin(\theta+\frac{\pi}{3})}} \frac{\tau}{(r+\theta)^2} r dr\, d\theta.$$

We get

$$\sum_{j=1}^{J} \iint_{\Delta_j} \sum_{i=1}^{3} p_r^{(j_i)}(x,y) \frac{1}{|\Omega'|} dx\, dy$$
$$= \iint_{\Delta_j} \sum_{i=1}^{3} p_r^{(j_i)}(x,y) \frac{J}{|\Omega'|} dx\, dy$$
$$= \frac{3}{|\Delta_j|} \iint_{\Delta} p_r^{(j_1)}(x,y) dx\, dy \qquad (17)$$
$$= \frac{3}{|\Delta_j|} \int_0^{\frac{\pi}{3}} \int_0^{\frac{3r_4}{2\sin(\theta+\frac{\pi}{3})}} \frac{\tau}{(r+\theta)^2} r dr\, d\theta$$
$$\geq \bar{p}_s.$$

Similar to the proof of Theorem 1, the average area over which a reader can provision sufficient energy for the WISP tags is no more than $\zeta/\bar{p}_s$, where ζ is given by

$$\zeta = \int_0^{2\pi} \int_0^{r_2} p_r(r) r dr\, d\theta$$
$$= 2\pi\tau \ln \frac{r_2+\beta}{\beta} - 2\pi\tau\beta \frac{r_2}{\beta(r_2+\beta)}.$$

Hence, we have $N_* \geq \frac{l_1 l_2 \bar{p}_s}{\zeta}$. Similarly, letting $S_4 = 3\sqrt{3}r_4^2/2$, we obtain

$$N_a \leq \frac{l_1 l_2}{S_4} + \frac{4r_4(l_1+l_2)+16r_4^2}{S_4},$$

which completes the proof by taking the limit of N_a/N_*.   □

Remarks.

1. *Because of the uniform node distribution, we transform the accumulative average power over the whole region Ω' into a subregion of an equilateral triangle, which brings great convenience to solving the problem. A similar process could be performed for other kinds of node distributions, but perhaps with added complexity.*
2. *Due to the exploitation of mobility, the approximation ratios can be closer to one than those in point provisioning, an observation that is supported by our simulation results.*
3. *When every point (x,y) inside the triangle Δ has a recharge power of $3p_r(x,y) \geq \bar{p}_s$ (as in point provisioning), it is obvious that*
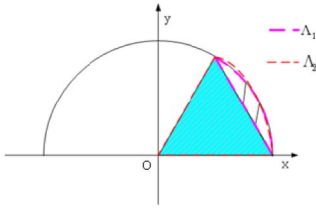
Fig. 6. An illustration for the integration of (18).

$$\frac{1}{|\Delta|}\iint_\Delta 3p_r(x,y)dx\,dy \geq \frac{\bar{p}_s}{|\Delta|}\iint_\Delta dx\,dy = \bar{p}_s.$$

Hence, $r_4 \geq r_3$. From this point of view, point provisioning can be regarded as a special conservative case of path provisioning. Fig. 4c gives an illustration.

4. *In Theorem 2, we do not have a closed-form formula for r_4. However, numerical methods can be employed to obtain an approximate r_4 [29]. For example, first we have*

$$\iint_\Delta p_r(x,y)dx\,dy$$

$$= \iint_{\Lambda_2 - \Lambda_1} p_r(x,y)dx\,dy$$

$$\geq \iint_{\Lambda_2} p_r(x,y)dx\,dy - \iint_{\Lambda_1} \frac{\tau}{\left(\frac{3r_4}{2} + \beta\right)^2} dx\,dy$$

$$= \frac{\pi\tau}{3}\left(\ln A + \frac{1}{A} - 1\right) - \frac{(\pi/2 - 3\sqrt{3}/4)r_4^2\tau}{(3r_4/2 + \beta)^2} \geq \frac{\bar{p}_s|\Delta|}{3},$$

$$(18)$$

where $A = \frac{\sqrt{3}r_4 + \beta}{\beta}$, and Λ_1 and Λ_2 are the regions shown in Fig. 6. The inequality holds because $\frac{3}{2}r_4$ is the minimum distance from the origin to the region Λ_1. Then, optimization methods can be applied to find the maximum value satisfying Inequality (18). Other approximation methods can be performed in a similar way.

5. *Although our derivation is based on the uniform distribution model of mobility, the proof process of Theorem 2 can obtain r_4 similarly for a general distribution $f(x,y)$. Specifically, we can use a numerical method such as the Monte Carlo method [30] to find r_4 satisfying the following inequality:*

$$\sum_{j=1}^J \iint_{\Delta_j} \sum_{i=1}^3 p_r^{(j_i)}(x,y)f(x,y)dx\,dy \geq \bar{p}_s. \quad (19)$$

7 SIMULATIONS

In this section, we report simulation results based on the settings of real WISP platforms. The main objective of our

simulations is to verify the analysis for *point provisioning* and *path provisioning*.

In the recharge model, $\tau = \frac{G_s G_r \eta}{L_p}(\frac{\lambda}{4\pi})^2 p_0$. From Section 4, we get $\tau = 4.32 \times 10^{-4}$ and $\beta = 0.2316$. The average current consumption for each sensor measurement and flash memory event is $500\,\mu A$ [13], respectively. The operation voltage is 2.2 V, and thus, $p_s = 2.2 \times 10^{-3}W$. Assume that the duration of each sensor measurement and flash memory event is 50 ms and the measurement cycle is denoted by T. Then, the average consumption power $\bar{p}_s = \frac{2.2 \times 10^{-4} + 3.96(T-0.1) \times 10^{-6}}{T}$, where 3.96×10^{-6} is the average power during sleep. Hence, the average consumption power $\bar{p}_s$ depends on the measurement cycle T, and their relationship is shown in Table 2. It is obvious from Table 2 that the longer the measurement cycle T, the less the average consumption power and the larger the parameter r_1. This implies that we should set T as large as possible to reduce the number of deployed readers, as long as application requirements are met.

7.1 Point Provisioning

We first evaluate the performance of point provisioning. We show r_3 under different T values also in Table 2. Clearly, r_3 is much larger than r_1 ($r_3 \approx 1.8r_1$). Hence, to provision energy for WISP tags in the same region Ω, the required number of readers in our approach is about 0.3 times of that required in the traditional triangular deployment approach, i.e., a 70 percent reduction. The results validate our conclusion that the proposed approach exploiting the additivity of recharge power has significantly higher efficiency compared with the traditional sensing disc model.

We proceed to discuss power distribution in the point provisioning. We take as an example $T = 8$, where the corresponding $r_3 = 6.19$. Consider a region of $50\,m \times 50\,m$. The readers are deployed according to Theorem 1. The available power at each point in the region is calculated, and the results are plotted in Fig. 7. We see that WISPs at points near a reader can collect abundant energy for operation, whereas the points of minimum recharge power (see the proof of Theorem 1) receive the lowest power distribution.

We proceed to evaluate the gap between our solution and the optimal solution. The parameter $\bar{p}_{th}$, the range beyond which WISP tags cannot harvest energy from readers, depends on the transmit power of readers and the hardware of WISP tags. We set $\bar{p}_{th} = 10^{-6}W$ in our simulations. The corresponding r_2 is 20.55 m. In Fig. 8, we plot numerical results of the upper bound asymptotic approximation ratio of the number of readers in our deployment to that in an optimal deployment, under

TABLE 2
Parameter Comparisons between Point Provisioning and Path Provisioning

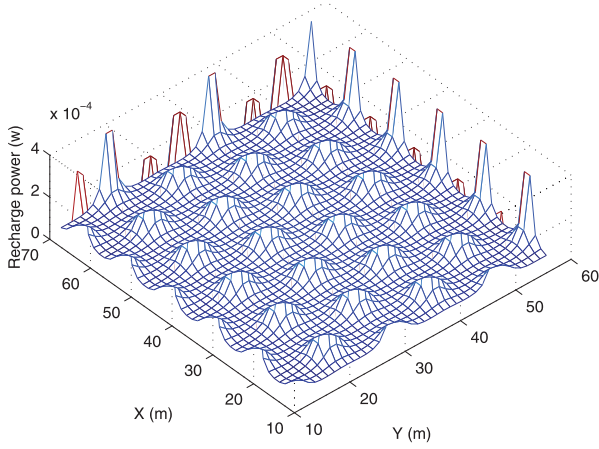| T (second)	1.6	2.4	3.2	4	4.8	5.6	6.4	7.2	8
r_1 (m)	1.52	1.90	2.21	2.48	2.72	2.93	3.13	3.31	3.48
r_3 (m)	2.80	3.45	4.00	4.46	4.87	5.25	5.59	5.90	6.19
r_4 (m)	4.22	5.37	6.34	7.19	7.95	8.64	9.28	9.88	10.43
$\bar{p}_s(W)$	1.41×10^{-4}	9.55×10^{-5}	7.26×10^{-5}	5.89×10^{-5}	4.97×10^{-5}	4.32×10^{-5}	3.83×10^{-5}	3.45×10^{-5}	3.14×10^{-5}

Fig. 7. Power distribution over a region of $50\text{ m} \times 50\text{ m}$ when the period $T = 8$ in the point provisioning.
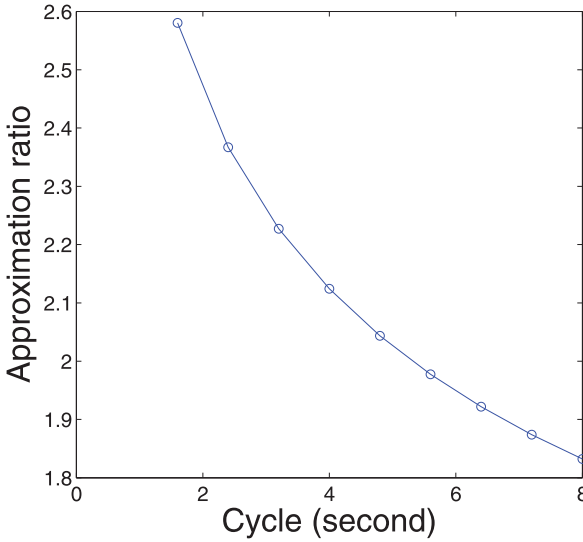
Fig. 8. Illustration of upper bound approximation ratio under different T in point provisioning.
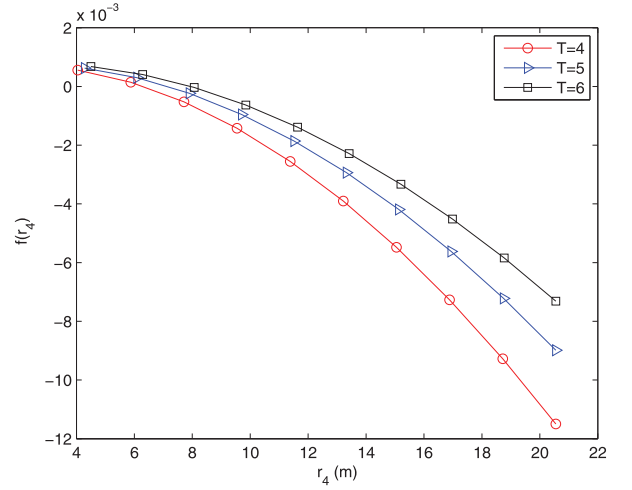

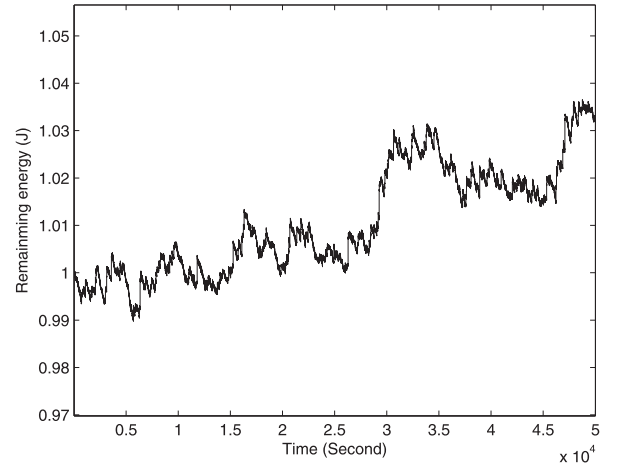Fig. 9. Values of $f(r_4)$ under $T = 4, 5, 6$ for different r_4.

Fig. 10. Remaining energy of a WISP tag traveling according to a uniform distribution model, within a region of $50\text{ m} \times 50\text{ m}$.

different T. It can be seen from Fig. 8 that the asymptotic ratio decreases as the cycle length T increases. When $T = 1.6$ s, the maximum ratio is 2.58. When $T = 8$ s, the minimum ratio is 1.83. Note that the reported asymptotic approximation ratio is a pessimistic estimate; the performance of our approach in practice can be even better. We conclude that the proposed deployment scheme is effective and achieves performance reasonably close to the optimal.

7.2 Path Provisioning

We now evaluate the performance of path provisioning. We start with showing how to find r_4 for path provisioning, i.e., find the largest r_4 satisfying (14). As mentioned in Section 6, we can use the approximation approach to obtain (18). Let $f(r_4) = \frac{\pi \tau}{3}(\ln A + \frac{1}{A} - 1) - \frac{(\pi/2 - 3\sqrt{3}/4)r_4^2 \tau}{(3r_4/2 + \beta)^2} - \frac{\bar{p}_s |\Delta|}{3}$. We plot the numerical results of $f(r_4)$ in Fig. 9. From Fig. 9, $f(\cdot)$ is a decreasing function of r_4. Hence, the root of the equation $f(r_4) = 0$ is the largest r_4 satisfying (18), which is easy to compute. We show the computed results for r_4 satisfying (18) in Table 2. Clearly, r_4 is much larger than r_3 due to mobility of the WISP tags. Hence, we conclude that

mobility can be exploited in WRSNs to significantly reduce the number of deployed readers.

We proceed to conduct simulations to evaluate the energy provisioning. As in point provisioning, we consider the region of $50\text{ m} \times 50\text{ m}$. Readers are deployed according to Theorem 2. A WISP tag travels within the region randomly according to uniform distribution. The period T is set to be 4 s. The initial energy of the tag is 1 J. During sleep, the WISP tag spends 3.96×10^{-6} J/s. Every T time, it becomes active to sense and log data, which consumes a total energy of 2.2×10^{-4} J. The values of total remaining energy at each second are recorded and plotted in Fig. 10. The remaining energy oscillates around 1 J over the operation time. However, the deviations are all less than 0.1 J. Hence, we conclude that the deployment can provision sufficient energy for the WISP tag traveling according to the uniform distribution model of mobility. We also record the values of energy collected at each second and plot them in Fig. 11. Most of the time, the tag is far from the readers, which results in a low recharge rate. When it gets close to one of the readers, however, it may receive a large amount of energy, which can be stored for further usage at the energy-starved points.

Lastly, we evaluate the gap between our solution and the optimal solution in the path provisioning. Results of the
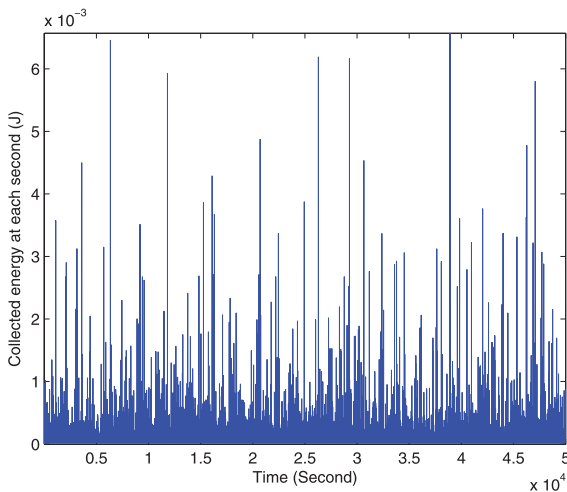
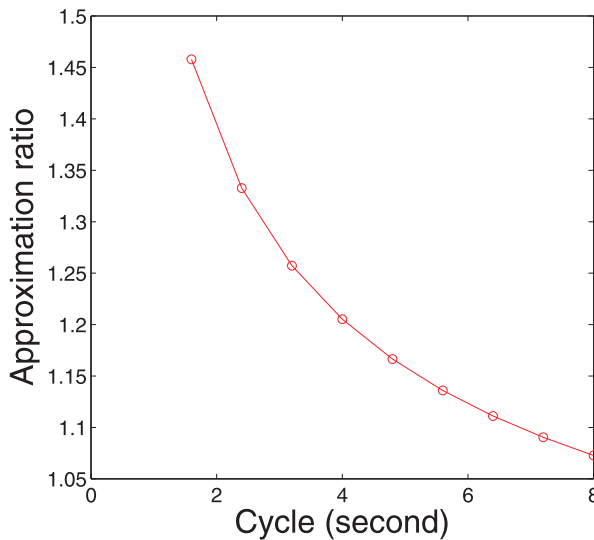Fig. 11. The energy collected by the WISP tag at each second.

Fig. 12. An illustration of upper bound approximation ratio under different T in path provisioning.

upper bound approximation ratio are plotted in Fig. 12. Note that the worst ratio is less than 1.5 and the best one is close to 1. Hence, our approach achieves practically close performance compared with the optimal.

8 CONCLUSION

In this paper, we study the energy provisioning problem in WRSNs. We propose an empirical recharge model based on experimental data. We investigate two forms of the problem: *point provisioning* and *path provisioning*. Additivity of recharge power from multiple readers is exploited to achieve an efficient deployment for *point provisioning*. The mobility of WISP tags can be further exploited to solve the *path provisioning* problem. For both problems, the upper bound asymptotic approximation ratios of the proposed solutions to the optimal ones are given analytically. Our analysis, supported by simulation results, show that our deployment methods can greatly reduce the number of readers compared with solutions based on traditional perfect disc sensing models.

REFERENCES

[1] I. Akyildiz, W. Su, Y. Sankarasubramaniam, and E. Cayirci, "A Survey on Sensor Networks," *IEEE Comm. Magazine,* vol. 40, no. 8, pp. 102-114, Aug. 2002.
[2] H. Nakayama, N. Ansari, A. Jamalipour, and N. Kato, "Fault-Resilient Sensing in Wireless Sensor Networks," *Computer Comm.,* vol. 30, nos. 11/12, pp. 2376-2384, 2007.
[3] K. Chebrolu, B. Raman, and N.M. BriMon, "A Sensor Network System for Railway Bridge Monitoring," *Proc. ACM MobiSys,* pp. 2-14, 2008.
[4] M. Buettner, R. Parsad, M. Philipose, and D. Wetherall, "Recognizing Daily Activities with RFID-Based Sensors," *Proc. ACM Int'l Conf. Ubiquitous Computing (UbiComp),* 2009.
[5] H. Liang, B.J. Choi, W. Zhuang, and X. Shen, "Towards Optimal Energy Store-Carry-and-Deliver for PHEVs via V2G System," *Proc. IEEE INFOCOM,* 2012.
[6] V. Raghunathan, A. Kansal, J. Hsu, J. Friedman, and M. Srivastava, "Design Considerations for Solar Energy Harvesting Wireless Embedded Systems," *Proc. Int'l Symp. Information Processing in Sensor Networks (IPSN),* 2005.
[7] S. Meninger, J. Mur-Miranda, and R. Amirtharajah, "Vibration-to-Electric Energy Conversion," *IEEE Trans. Very Large Scale Integration Systems,* vol. 9, no. 1, pp. 64-76, Feb. 2001.
[8] I. Stark, "Thermal Energy Harvesting with Thermo Life," *Proc. Int'l Workshop Wearable and Implantable Body Sensor Networks,* 2006.
[9] C. Park and P. Chou, "AmbiMax: Autonomous Energy Harvesting Platform for Multi-Supply Wireless Sensor Nodes," *Proc. IEEE Comm. Soc. Conf. Sensor, Mesh and Ad Hoc Comm. and Networks (SECON),* 2006.
[10] E. Thomson, "Preventing Forest Fires with Tree Power: Sensor System Runs on Electricity Generated by Trees," http://www.physorg.com/news141291261.html, 2008.
[11] T. Starner, "Human-Powered Wearable Computing," *IBM Systems J.,* vol. 35, pp. 618-629, 1996.
[12] A. Kurs, A. Karalis, R. Moffatt, J. Joannopoulos, P. Fisher, and M. Soljačić, "Wireless Power Transfer via Strongly Coupled Magnetic Resonances," *Science,* vol. 9, no. 1, pp. 64-76, 2001.
[13] D. Yeager, P. Powledge, R. Prasad, D. Wetherall, and J. Smith, "Wirelessly-Charged UHF Tags for Sensor Data Collection," *Proc. IEEE Int'l Conf. Radio Frequency Identification (RFID '08),* 2008.
[14] A. Juels, "RFID Security and Privacy: A Research Survey," *IEEE J. Selected Areas in Comm.,* vol. 24, no. 2, pp. 381-394, Feb. 2006.
[15] A. Sample, D. Yaniel, P. Powledge, A. Mamishev, and J. Smith, "Design of an RFID-Based Battery-Free Programmable Sensing Platform," *IEEE Trans. Instrumentation and Measurement,* vol. 57, no. 11, pp. 2608-2615, Nov. 2008.
[16] M. Philipose, J. Smith, B. Jiang, K. Sundara-Rajan, A. Mamishev, and S. Roy, "Battery-Free Wireless Identification and Sensing," *IEEE Pervasive Computing,* vol. 4, no. 1, pp. 37-45, Jan.-Mar. 2005.
[17] M. Buettner, B. Greenstein, A. Sample, and J. Smith, "Revisiting Smart Dust with RFID Sensor Networks Michael Buettner," *Proc. ACM Workshop Hot Topics in Networks (HotNets-VII),* 2008.
[18] A. Sample, D. Yeager, and J. Smith, "A Capacitive Touch Interface for Passive RFID Tags," *Proc. IEEE Int'l Conf. Radio Frequency Identification (RFID '09),* 2009.
[19] G. Xing, X. Wang, Y. Zhang, C. Lu, R. Pless, and C. Gill, "Integrated Coverage and Connectivity Configuration in Wireless Sensor Networks," *ACM Trans. Sensor Networks,* vol. 1, no. 1, pp. 36-72, 2005.

[20] B. Liu, P. Brass, O. Dousse, P. Nain, and D. Towsley, "Mobility Improves Coverage of Sensor Networks," *Proc. ACM MobiHoc,* 2005.

[21] R. Kershner, "The Number of Circles Covering a Set," *Am. J. Math.,* vol. 61, no. 3, pp. 665-671, 1939.

[22] H. Zhang and J. Hou, "Maintaining Sensing Coverage and Connectivity in Large Sensor Networks," *Proc. Int'l Workshop Theoretical and Algorithmic Aspects of Sensor, Ad Hoc Wireless, and Peer-to-Peer Networks,* 2004.

[23] B. Wang, V. Srinivasan, K. Chua, and W. Wang, "Information Coverage in Randomly Deployed Wireless Sensor Networks," *IEEE Trans. Wireless Comm.,* vol. 6, no. 8, pp. 2994-3004, Aug. 2007.

[24] G. Yang and D. Qiao, "Barrier Information Coverage with Wireless Sensors," *Proc. IEEE INFOCOM,* 2009.

[25] M. Hefeeda and H. Ahmadi, "A Probabilistic Coverage Protocol for Wireless Sensor Networks," *Proc. IEEE Int'l Conf. Network Protocols (ICNP '07),* 2007.

[26] X. Bai, S. Kumar, D. Xuan, Z. Yun, and T. Lai, "Deploying Wireless Sensors to Achieve Both Coverage and Connectivity," *Proc. ACM MobiHoc,* 2006.

[27] C. Hsin and M. Liu, "Network Coverage Using Low Duty-Cycled Sensors: Random and Coordinated Sleep Algorithms," *Proc. Int'l Symp. Information Processing in Sensor Networks (IPSN),* 2004.

[28] C. Bettstetter, G. Resta, and P. Santi, "The Node Distribution of the Random Waypoint Mobility Model for Wireless Ad Hoc Networks," *IEEE Trans. Mobile Computing,* vol. 2, no. 3, pp. 257-269, July-Sept. 2003.

[29] P. Davis and P. Rabinowitz, *Methods of Numerical Integration.* Academic, 1975.

[30] R. Rubinstein and D. Kroese, *Simulation and the Monte Carlo Method.* Wiley, 2008.
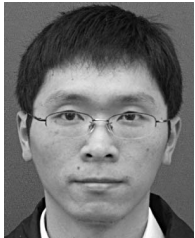
Shibo He received the PhD degree in control science and engineering from Zhejiang University in 2012. He is a member of the Group of Networked Sensing and Control (IIPC-nesC) in the State Key Laboratory of Industrial Control Technology at Zhejiang University. His research interests include coverage, cross-layer optimization, and distributed algorithm design problems in wireless sensor networks.

Jiming Chen received the BSc and PhD degrees both in control science and engineering from Zhejiang University in 2000 and 2005, respectively. He was a visiting researcher at INRIA in 2006, at the National University of Singapore in 2007, and at the University of Waterloo from 2008 to 2010. He is currently a full professor in the Department of Control Science and Engineering and the coordinator of the Group of Networked Sensing and Control in the State Key Laboratory of Industrial Control Technology at Zhejiang University, China. His research interests are in estimation and control over sensor networks, sensor and actuator networks, and coverage and optimization in sensor networks. He currently serves as an associate editor for several international journals including the *IEEE Transactions on Industrial Electronics.* He is has been a guest editor of the *IEEE Transactions on Automatic Control*, *Computer Communication* (Elsevier), *Wireless Communication and Mobile Computer* (Wiley), and the *Journal of Network and Computer Applications* (Elsevier). He has also served as a cochair for the Ad Hoc and Sensor Network Symposium and IEEE GlobeCom 2011, general symposia cochair of ACM IWCMC 2009 and ACM IWCMC 2010, MAC track cochair of WiCON 2010, publicity cochair of IEEE MASS 2011, IEEE DCOSS 2011, and IEEE ICDCS 2012, and TPC member for IEEE ICDCS 2010, IEEE MASS 2010, IEEE SECON 2011, IEEE INFOCOM 2011, IEEE INFOCOM 2012, and IEEE ICDCS 2012. He is a senior member of the IEEE.

Fachang Jiang is currently working toward the master's degree in control science and engineering at Zhejiang University, Hangzhou, China. He is a member of the Group of Networked Sensing and Control (IIPC-nesC) in the State Key Laboratory of Industrial Control Technology at Zhejiang University. His research interests include hardware system design in rechargeable sensor networks.

David K.Y. Yau received the BSc degree (first class honors) from the Chinese University of Hong Kong, and the MS and PhD degrees from the University of Texas at Austin, all in computer science. He is currently a distinguished scientist in the Advanced Digital Sciences Center, Singapore, and an associate professor of computer science at Purdue University, West Lafayette, Indiana. He received the US National Science Foundation CAREER award for research in quality of service provisioning. His other areas of research interest are protocol design and implementation, wireless and sensor networks, network security, network incentives, and smart grids. He served as an associate editor of the *IEEE/ACM Transactions on Networking* (2004-2009); vice general chair (2006), TPC cochair (2007), and TPC area chair (2011) of the IEEE International Conference on Network Protocols; TPC cochair (2006) and steering committee member (2007-2009) of the IEEE International Workshop Quality of Service; and TPC track cochair (network/web/P2P protocols and applications) of the IEEE International Conference Distributed Computing Systems (2012). He is a member of the IEEE.

Guoliang Xing received the BS degree in electrical engineering and the MS degree in computer science from Xi'an Jiao Tong University, China, in 1998 and 2001, respectively. He received the MS and DSc degrees in computer science and engineering from Washington University, St. Louis, in 2003 and 2006, respectively. He is an assistant professor in the Department of Computer Science and Engineering at Michigan State University. From 2006 to 2008, he was an assistant professor of computer science, City University of Hong Kong. He served on a number of technical program committees and held several workshop organization positions including program cochair of the First ACM International Workshop on Heterogeneous Sensor and Actor Networks (HeterSanet) 2008 and the Workshop on Wireless Ad hoc and Sensor Networks 2008 and 2009. His research interests include power management and controlled mobility in wireless sensor networks, data fusion-based network design and analysis, and cyber-physical systems. He is a member of the IEEE.

Youxian Sun received a diploma from the Department of Chemical Engineering, Zhejiang University, China, in 1964. He joined the Department of Chemical Engineering, Zhejiang University in 1964. From 1984 to 1987, he was an Alexander Von Humboldt research fellow and visiting associate professor at the University of Stuttgart, Germany. He has been a full professor at Zhejiang University since 1988. In 1995, he was promoted to an academician of the Chinese Academy of Engineering. His current research interests include modeling, control, and optimization of complex systems, and robust control design and its application. He is author/coauthor of 450 journal and conference papers. He is currently the director of the Institute of Industrial Process Control and the National Engineering Research Center of Industrial Automation, Zhejiang University. He is the president of the Chinese Association of Automation and has also served as the vice-chairman of the IFAC Pulp and Paper Committee and the vice-president of China Instrument and Control Society.